

Observation of $B^\pm \rightarrow p\bar{p}K^\pm$

K. Abe⁹, K. Abe⁴⁰, R. Abe³⁰, T. Abe⁴¹, I. Adachi⁹, Byoung Sup Ahn¹⁷, H. Aihara⁴², M. Akatsu²³, Y. Asano⁴⁷, T. Aso⁴⁶, V. Aulchenko², T. Aushev¹⁴, A. M. Bakich³⁷, Y. Ban³⁴, E. Banas²⁸, S. Behari⁹, P. K. Behera⁴⁸, A. Bondar², A. Bozek²⁸, M. Bračko^{21,15}, J. Brodzicka²⁸, T. E. Browder⁸, B. C. K. Casey⁸, P. Chang²⁷, Y. Chao²⁷, K.-F. Chen²⁷, B. G. Cheon³⁶, R. Chistov¹⁴, S.-K. Choi⁷, Y. Choi³⁶, M. Danilov¹⁴, L. Y. Dong¹², J. Dragic²², A. Drutskoy¹⁴, S. Eidelman², V. Eiges¹⁴, Y. Enari²³, C. W. Everton²², F. Fang⁸, H. Fujii⁹, C. Fukunaga⁴⁴, M. Fukushima¹¹, N. Gabyshev⁹, A. Garmash^{2,9}, T. Gershon⁹, K. Gotow⁴⁹, R. Guo²⁵, J. Haba⁹, H. Hamasaki⁹, F. Handa⁴¹, K. Hara³², T. Hara³², H. Hayashii²⁴, M. Hazumi⁹, E. M. Heenan²², I. Higuchi⁴¹, T. Higuchi⁴², T. Hojo³², T. Hokuue²³, Y. Hoshi⁴⁰, S. R. Hou²⁷, W.-S. Hou²⁷, H.-C. Huang²⁷, T. Igaki²³, Y. Igarashi⁹, H. Ikeda⁹, K. Inami²³, A. Ishikawa²³, H. Ishino⁴³, R. Itoh⁹, H. Iwasaki⁹, Y. Iwasaki⁹, P. Jaloča²⁸, H. K. Jang³⁵, J. H. Kang⁵⁰, J. S. Kang¹⁷, P. Kapusta²⁸, N. Katayama⁹, H. Kawai³, H. Kawai⁴², Y. Kawakami²³, N. Kawamura¹, T. Kawasaki³⁰, H. Kichimi⁹, D. W. Kim³⁶, H. J. Kim⁵⁰, H. O. Kim³⁶, Hyunwoo Kim¹⁷, S. K. Kim³⁵, K. Kinoshita⁵, H. Konishi⁴⁵, S. Korpar^{21,15}, P. Križan^{20,15}, P. Krokovny², S. Kumar³³, A. Kuzmin², Y.-J. Kwon⁵⁰, J. S. Lange⁶, G. Leder¹³, S. H. Lee³⁵, A. Limosani²², D. Liventsev¹⁴, R.-S. Lu²⁷, J. MacNaughton¹³, G. Majumder³⁸, F. Mandl¹³, T. Matsuishi²³, S. Matsumoto⁴, Y. Mikami⁴¹, W. Mitaroff¹³, K. Miyabayashi²⁴, Y. Miyabayashi²³, H. Miyake³², H. Miyata³⁰, G. R. Moloney²², T. Nagamine⁴¹, Y. Nagasaka¹⁰, Y. Nagashima³², M. Nakao⁹, J. W. Nam³⁶, Z. Natkaniec²⁸, S. Nishida¹⁸, O. Nitoh⁴⁵, S. Noguchi²⁴, T. Nozaki⁹, S. Ogawa³⁹, T. Ohshima²³, T. Okabe²³, S. Okuno¹⁶, S. L. Olsen⁸, W. Ostrowicz²⁸, H. Ozaki⁹, P. Pakhlov¹⁴, H. Palka²⁸, C. S. Park³⁵, C. W. Park¹⁷, K. S. Park³⁶, L. S. Peak³⁷, J.-P. Perroud¹⁹, M. Peters⁸, L. E. Piiilonen⁴⁹, F. Ronga¹⁹, N. Root², K. Rybicki²⁸, H. Sagawa⁹, Y. Sakai⁹, H. Sakamoto¹⁸, M. Satapathy⁴⁸, A. Satpathy^{9,5}, O. Schneider¹⁹, S. Schrenk⁵, C. Schwanda^{9,13}, S. Semenov¹⁴, K. Senyo²³, H. Shibuya³⁹, B. Shwartz², V. Sidorov², J. B. Singh³³, S. Stanič⁴⁷, A. Sugi²³, A. Sugiyama²³, K. Sumisawa⁹, K. Suzuki⁹, S. Y. Suzuki⁹, T. Takahashi³¹, F. Takasaki⁹, M. Takita³², K. Tamai⁹, N. Tamura³⁰, J. Tanaka⁴², G. N. Taylor²², Y. Teramoto³¹, S. Tokuda²³, T. Tomura⁴², S. N. Tovey²², K. Trabelsi⁸, T. Tsuboyama⁹, T. Tsukamoto⁹, S. Uehara⁹, K. Ueno²⁷, Y. Unno³, S. Uno⁹, K. E. Varvell³⁷, C. C. Wang²⁷, C. H. Wang²⁶, J. G. Wang⁴⁹, M.-Z. Wang²⁷, Y. Watanabe⁴³, E. Won³⁵, B. D. Yabsley⁹, Y. Yamada⁹, M. Yamaga⁴¹, A. Yamaguchi⁴¹, H. Yamamoto⁴¹, Y. Yamashita²⁹, M. Yamauchi⁹, S. Yanaka⁴³, P. Yeh²⁷, M. Yokoyama⁴², Y. Yuan¹², J. Zhang⁴⁷, Y. Zheng⁸, and D. Žontar⁴⁷

(Belle Collaboration)

¹Aomori University, Aomori

²Budker Institute of Nuclear Physics, Novosibirsk

³Chiba University, Chiba

⁴Chuo University, Tokyo

⁵University of Cincinnati, Cincinnati OH

⁶University of Frankfurt, Frankfurt

⁷Gyeongsang National University, Chinju

⁸University of Hawaii, Honolulu HI

⁹High Energy Accelerator Research Organization (KEK), Tsukuba

¹⁰Hiroshima Institute of Technology, Hiroshima

¹¹Institute for Cosmic Ray Research, University of Tokyo, Tokyo

¹²Institute of High Energy Physics, Chinese Academy of Sciences, Beijing

¹³Institute of High Energy Physics, Vienna

¹⁴Institute for Theoretical and Experimental Physics, Moscow

¹⁵J. Stefan Institute, Ljubljana

¹⁶Kanagawa University, Yokohama

¹⁷Korea University, Seoul

¹⁸Kyoto University, Kyoto

¹⁹IPHE, University of Lausanne, Lausanne

²⁰University of Ljubljana, Ljubljana

²¹University of Maribor, Maribor

²²University of Melbourne, Victoria

²³Nagoya University, Nagoya

²⁴Nara Women's University, Nara

²⁵National Kaohsiung Normal University, Kaohsiung

²⁶National Lien-Ho Institute of Technology, Miao Li

²⁷National Taiwan University, Taipei

²⁸H. Niewodniczanski Institute of Nuclear Physics, Krakow

- ²⁹Nihon Dental College, Niigata
- ³⁰Niigata University, Niigata
- ³¹Osaka City University, Osaka
- ³²Osaka University, Osaka
- ³³Panjab University, Chandigarh
- ³⁴Peking University, Beijing
- ³⁵Seoul National University, Seoul
- ³⁶Sungkyunkwan University, Suwon
- ³⁷University of Sydney, Sydney NSW
- ³⁸Tata Institute of Fundamental Research, Bombay
- ³⁹Toho University, Funabashi
- ⁴⁰Tohoku Gakuin University, Tagajo
- ⁴¹Tohoku University, Sendai
- ⁴²University of Tokyo, Tokyo
- ⁴³Tokyo Institute of Technology, Tokyo
- ⁴⁴Tokyo Metropolitan University, Tokyo
- ⁴⁵Tokyo University of Agriculture and Technology, Tokyo
- ⁴⁶Toyama National College of Maritime Technology, Toyama
- ⁴⁷University of Tsukuba, Tsukuba
- ⁴⁸Utkal University, Bhubaneswer
- ⁴⁹Virginia Polytechnic Institute and State University, Blacksburg VA
- ⁵⁰Yonsei University, Seoul

We report the observation of the decay mode $B^\pm \rightarrow p\bar{p}K^\pm$ based on an analysis of 29.4 fb^{-1} of data collected by the Belle detector at KEKB. This is the first example of a $b \rightarrow s$ transition with baryons in the final state. The $p\bar{p}$ mass spectrum in this decay is inconsistent with phase space and is peaked at low mass. The branching fraction for this decay is measured to be $\mathcal{B}(B^\pm \rightarrow p\bar{p}K^\pm) = (4.3_{-0.9}^{+1.1}(\text{stat}) \pm 0.5(\text{syst})) \times 10^{-6}$. We also report upper limits for the decays $B^0 \rightarrow p\bar{p}K_S$ and $B^\pm \rightarrow p\bar{p}\pi^\pm$.

PACS numbers: 13.20.He, 13.25.Hw, 13.60.Rj

We report the results of searches for the decay modes $B^+ \rightarrow p\bar{p}K^+$ [1] and $B^0 \rightarrow p\bar{p}K_S$. These modes are expected to proceed mainly via $b \rightarrow s$ penguin diagrams. We also search for $B^+ \rightarrow p\bar{p}\pi^+$ which is expected to occur primarily via a $b \rightarrow u$ tree process. Once they are established, these baryonic modes may be used to either constrain or observe direct CP violation in B decay [2].

In contrast to charm meson decay, final states with baryons are allowed in B meson decay. To date, a few low multiplicity B decay modes with baryons in the final state from $b \rightarrow c$ transitions have been observed [3]. Rare B decays due to charmless $b \rightarrow s$ and $b \rightarrow u$ transitions should also lead to final states with baryons. A number of searches for such modes have been carried out by CLEO [4], ARGUS [5], and LEP [6] but only upper limits were obtained. Stringent upper limits for two-body modes such as $B^0 \rightarrow p\bar{p}$, $B^+ \rightarrow \bar{\Lambda}p$ and $B^0 \rightarrow \Lambda\bar{\Lambda}$ have recently been reported by Belle [7].

We use a 29.4 fb^{-1} data sample, which contains 31.9 million produced $B\bar{B}$ pairs, collected with the Belle detector at the KEKB asymmetric-energy e^+e^- (3.5 on 8 GeV) collider [8]. KEKB operates at the $\Upsilon(4S)$ resonance ($\sqrt{s} = 10.58 \text{ GeV}$) with a peak luminosity that exceeds $5 \times 10^{33} \text{ cm}^{-2}\text{s}^{-1}$. The Belle detector is a large-solid-angle magnetic spectrometer that consists of a three-layer silicon vertex detector (SVD), a 50-layer central drift chamber (CDC), a mosaic of aerogel threshold Čerenkov counters (ACC), time-of-flight scintillation counters (TOF), and an array of CsI(Tl) crystals (ECL) located inside a superconducting solenoid coil that provides a 1.5 T magnetic field. An iron flux-return located outside of the coil is instrumented to identify K_L and muons (KLM). The detector is described in detail elsewhere [9].

We select well measured charged tracks with impact parameters with respect to the interaction point of less than 0.3 cm in the radial direction and less than 3 cm in the beam direction (z). These tracks are required to have $p_T > 50 \text{ MeV}/c$.

Particle identification likelihoods for each particle hypothesis are calculated by combining information from the TOF, ACC system with dE/dx measurements in the CDC. Protons and anti-protons are identified using all particle ID systems and are required to have proton likelihood ratios ($L_p/(L_p + L_K)$ and $L_p/(L_p + L_\pi)$) greater than 0.6. Proton candidates that are electron-like according to the information recorded by the CsI(Tl) calorimeter are vetoed. This selection is 89% efficient for protons with a 7% kaon misidentification rate. To identify kaons (pions), we require the kaon (pion) likelihood ratio to be greater than 0.6. This requirement is 88% efficient for kaons with a 8.5% misidentification rate for pions. In addition, we remove kaon candidates that are consistent with being protons.

For the $B^0 \rightarrow p\bar{p}K_S$ mode, we select K_S candidates from $\pi^+\pi^-$ candidates that lie within the mass window $0.482 \text{ GeV}/c^2 < M(\pi^+\pi^-) < 0.514 \text{ GeV}/c^2 (\pm 4\sigma)$. The distance of closest approach between the two daughter tracks is required to be less than 2.4 cm. The impact parameter of each track in the radial direction should have magnitude greater than 0.02 cm, and the flight length should be greater than 0.22 cm. The difference in the angle between the vertex direction and the K_S flight direction in the $x-y$ plane is required to satisfy $\Delta\phi < 0.03 \text{ rad}$.

To reconstruct signal candidates in the $B^+ \rightarrow p\bar{p}K^+$ mode, we form combinations of a kaon, proton and anti-proton that are inconsistent with the following $b \rightarrow c\bar{c}s$ transitions: $B^+ \rightarrow J/\psi K^+$, $J/\psi \rightarrow p\bar{p}$; $B^+ \rightarrow \eta_c K^+$, $\eta_c \rightarrow p\bar{p}$; $B^+ \rightarrow \psi' K^+$, $\psi' \rightarrow p\bar{p}$ and $B^+ \rightarrow \chi_{c[0,1]} K^+$, $\chi_{c[0,1]} \rightarrow p\bar{p}$. This set of requirements is referred to as the charm veto [10]. Similar charm vetoes are applied in the analysis of the other decay modes. In the case of $B^0 \rightarrow p\bar{p}K_S$, events with pK_S or $\bar{p}K_S$ masses consistent with the Λ_c are rejected.

To isolate the signal, we form the beam-constrained mass, $M_{bc} = \sqrt{E_{\text{beam}}^2 - \vec{P}_{\text{recon}}^2}$, and energy difference $\Delta E = E_{\text{recon}} - E_{\text{beam}}$ in the $\Upsilon(4S)$ center of mass frame. Here E_{beam} , E_{recon} and \vec{P}_{recon} are the beam energy, the reconstructed energy and the reconstructed momentum of the signal candidate, respectively. The signal region for ΔE is $\pm 50 \text{ MeV}$ which corresponds to $\pm 5\sigma$ where σ is the resolution determined from a Gaussian fit to the Monte Carlo (MC) simulation. The signal region for M_{bc} is $5.270 \text{ GeV}/c^2 < M_{bc} < 5.290 \text{ GeV}/c^2$. The resolution in beam-constrained mass is $2.8 \text{ MeV}/c^2$ and is dominated by the beam energy spread of KEKB.

Several event topology variables provide discrimination between the large continuum ($e^+e^- \rightarrow q\bar{q}$, where $q = u, d, s, c$) background, which tends to be collimated along the original quark direction, and more spherical $B\bar{B}$ events. We form a likelihood ratio using two variables. Six modified Fox-Wolfram moments and the cosine of the thrust angle are combined into a Fisher discriminant [11]. For signal MC and continuum data, we then form probability density functions for this Fisher discriminant, and the cosine of the B decay angle with respect to the z axis ($\cos\theta_B$). The signal (background) probability density functions are multiplied together to form a signal (background) likelihood \mathcal{L}_S (\mathcal{L}_{BG}). The likelihood ratio $\mathcal{L}_S/(\mathcal{L}_S + \mathcal{L}_{BG})$ is then required to be greater than 0.6. The event topology requirements retain 78% of the signal while removing 87% of the continuum background.

In Fig. 1, we show the ΔE and beam-constrained mass distributions for the signal candidates. We fit the ΔE distribution with a double Gaussian for signal and a linear background function with slope determined from the M_{bc}

sideband. The mean of the Gaussian is determined from $\bar{B}^0 \rightarrow \Lambda_c \bar{p} \pi^+ \pi^-$, $\Lambda_c \rightarrow p K^- \pi^+$ decays. The fit to the ΔE distribution gives a yield of $42.8_{-9.6}^{+10.8}$ with a significance of 5.6 standard deviations. In the fit to the ΔE distribution, the region with $\Delta E < -120$ MeV is excluded to avoid feed-downs from modes such as $B \rightarrow p \bar{p} K^*$. As a consistency check, we fit the M_{bc} distribution to the sum of a signal Gaussian and a background function with kinematic threshold. The width of the Gaussian is fixed from MC simulation while the mean is determined from $B^+ \rightarrow \bar{D}^0 \pi^+$ data. The shape parameter of the background function is determined from ΔE sideband data. In the M_{bc} distribution, we observe a signal of $42.9_{-9.1}^{+9.8}$ events. The signal yields and the branching fractions are determined from fits to the ΔE distribution rather than M_{bc} to minimize possible biases from $B\bar{B}$ background which tends to peak in M_{bc} but not in ΔE .

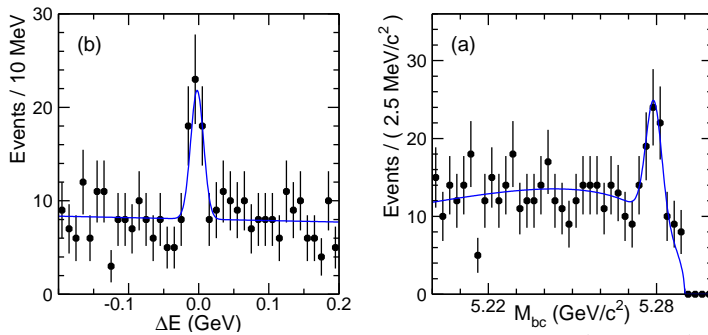


FIG. 1. (a) ΔE and (b) M_{bc} distributions for $B^+ \rightarrow p \bar{p} K^+$ candidates.

The background in these modes is predominantly due to continuum events. To check for $B\bar{B}$ backgrounds that might peak in the signal region, we used two large $B\bar{B}$ MC samples that correspond to an integrated luminosity that is about twice the size of the data sample. The estimated background is of order one event and no backgrounds that peak in the ΔE signal region were found. We also examined dedicated MC samples of $b \rightarrow c$ decay modes with baryons in the final state. We restricted our attention to low multiplicity decay modes. We generated samples of $\bar{B}^0 \rightarrow \Lambda_c^+ \bar{p}$, $B^- \rightarrow \Lambda_c^+ \bar{p} \pi^-$ and $B^- \rightarrow \Lambda_c^+ \bar{p} e^- \bar{\nu}_e$ that correspond to an integrated luminosity about a factor of ten larger than the data sample used here. The Λ_c charmed baryon was allowed to decay into all measured decay modes that contain a proton. Again no peaking backgrounds were observed.

We also examine the $M(p\bar{p})$ mass distributions for events in the ΔE , M_{bc} signal region. The signal yield as a function of $p\bar{p}$ mass is shown in Fig. 2. These yields were determined by fits to the ΔE distribution in bins of $p\bar{p}$ invariant mass. The distribution from a three-body phase space MC normalized to the area of the signal is superimposed. It is clear that the observed mass distri-

bution is not consistent with three-body phase space but instead is peaked at low $p\bar{p}$ mass. We also examine the pK^- mass distribution but do not observe any obvious narrow structures such as the $\Lambda(1520)$.

To avoid model dependence in the determination of the branching fraction for $p\bar{p}K^+$, we fit the ΔE signal yield in bins of $M(p\bar{p})$ and correct for the detection efficiency in each bin using a three-body phase space $B^+ \rightarrow p\bar{p}K^+$ MC model. The results of the fits are given in Table I. We then sum the partial branching fractions in each bin to obtain

$$\mathcal{B}(B^+ \rightarrow p\bar{p}K^+) = (4.3_{-0.9}^{+1.1}(\text{stat}) \pm 0.5(\text{syst})) \times 10^{-6}.$$

For $M(p\bar{p}) < 3.4$ GeV/c^2 , the mass region below the χ_c and ψ' resonances, $\mathcal{B}(B^+ \rightarrow p\bar{p}K^+) = (4.4_{-0.8}^{+1.0}(\text{stat}) \pm 0.5(\text{syst})) \times 10^{-6}$ with the charm veto applied. For $M(p\bar{p}) < 2.8$ GeV/c^2 , the region below charm threshold, we obtain $\mathcal{B}(B^+ \rightarrow p\bar{p}K^+) = (3.9_{-0.7}^{+0.9}(\text{stat}) \pm 0.4(\text{syst})) \times 10^{-6}$.

TABLE I. Fit results in bins of $M(p\bar{p})$. The detection efficiency (ϵ_{detect}) and the partial branching fraction (\mathcal{B}) for each bin are also listed.

$M(p\bar{p})(\text{GeV}/c^2)$	ΔE yield	ϵ_{detect}	$\mathcal{B}(\times 10^{-6})$
< 2.0	$10.2_{-3.7}^{+4.4}$	0.33	$0.97_{-0.35}^{+0.42}$
2.0-2.2	$7.8_{-3.4}^{+4.2}$	0.34	$0.73_{-0.32}^{+0.39}$
2.2-2.4	$11.9_{-3.9}^{+4.6}$	0.30	$1.24_{-0.41}^{+0.48}$
2.4-2.6	$5.5_{-3.0}^{+3.7}$	0.29	$0.61_{-0.33}^{+0.41}$
2.6-2.8	$3.3_{-2.3}^{+3.1}$	0.30	$0.34_{-0.24}^{+0.32}$
2.8-3.4	$4.6_{-2.7}^{+3.5}$	0.29	$0.50_{-0.29}^{+0.38}$
3.4-4.0	$-1.2_{-2.2}^{+2.5}$	0.27	$-0.14_{-0.25}^{+0.29}$
4.0-4.8	$0.3_{-2.8}^{+3.5}$	0.25	$0.04_{-0.36}^{+0.45}$

The contributions to the systematic error for the $B^+ \rightarrow p\bar{p}K^+$ mode are the uncertainties due to the tracking efficiency (6%), particle identification efficiency (8%) and the modeling of the likelihood ratio cut (2.6%). The particle identification systematic includes contributions of 3% for the proton and anti-proton and 2% for the charged kaon. The error in proton/anti-proton identification is determined using $\Lambda/\bar{\Lambda}$ samples, while the error in kaon identification efficiency is obtained from kinematically selected $D^{*+} \rightarrow D^0 \pi^+$, $D^0 \rightarrow K^- \pi^+$ in the data. The systematic error due to the modeling of the likelihood ratio cut is determined using $B^+ \rightarrow \bar{D}^0 \pi^+$ events reconstructed in data. The systematic error in the yield of the ΔE fit (3.8%) was determined by varying the mean and σ of the signal and the shape parameter of the background. The sources of systematic error are combined in quadrature to obtain the final systematic error of 11.0%.

For events in the ΔE , M_{bc} signal region we examine the proton, anti-proton and kaon particle identification likelihood distributions and compare to signal MC simulation. No discrepancy is observed. We also verify that

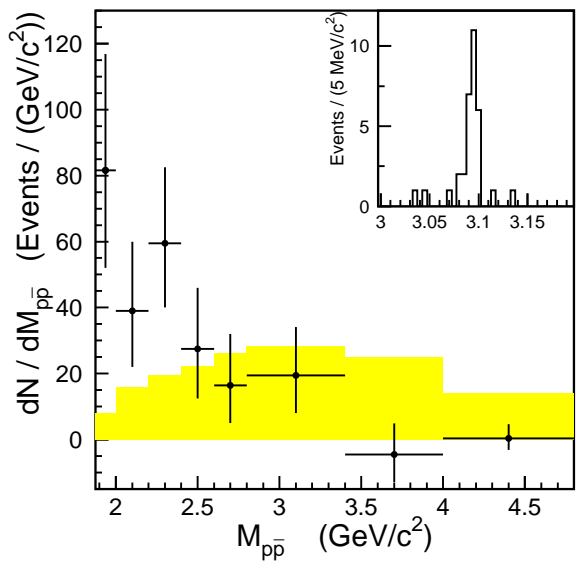


FIG. 2. The fitted yield divided by the bin size for $B^+ \rightarrow p\bar{p}K^+$ as a function of $p\bar{p}$ mass. The charm veto is applied. The distribution from non-resonant $B^+ \rightarrow p\bar{p}K^+$ MC simulation is superimposed. The inset shows the $p\bar{p}$ mass distribution for the $J/\psi K^+$ signal region.

the ECL shower width distribution is consistent with MC expectations for the proton and anti-proton candidates. In addition, we check the branching fraction as the cuts on the proton and anti-proton probabilities and likelihood ratio are varied. We do not observe any systematic trends beyond statistics.

To verify the analysis procedure and branching fraction determination, we remove the J/ψ veto and examine the decay chain $B^+ \rightarrow J/\psi K^+$, $J/\psi \rightarrow p\bar{p}$. A clear signal of 26.4 ± 5.2 events is then observed in the ΔE spectrum. We also observe 25.9 ± 5.1 events in the M_{bc} distribution. The $p\bar{p}$ invariant mass spectrum for $J/\psi K^+$ signal candidates is shown as an inset in Fig. 2. We use the ΔE yield and the MC detection efficiency of 0.30 to determine the branching fraction $\mathcal{B}(B^+ \rightarrow J/\psi K^+) = (13.1 \pm 2.6) \times 10^{-4}$. This is in good agreement with the PDG world average, $\mathcal{B}(B^+ \rightarrow J/\psi K^+) = (10.0 \pm 1.0) \times 10^{-4}$ [12], which was obtained by experiments that reconstruct the J/ψ in dilepton modes.

We also examined two related decay modes $B^0 \rightarrow p\bar{p}K_S$ and $B^+ \rightarrow p\bar{p}\pi^+$ that may help clarify the interpretation of the signal. Measurement of $B^0 \rightarrow p\bar{p}K_S$ will help to determine the role of the spectator quark in $b \rightarrow s$ decays with baryons, while observation of $B^+ \rightarrow p\bar{p}\pi^+$ will constrain the ratio of the $b \rightarrow u$ tree and $b \rightarrow s$ penguin diagrams in decays with baryons.

For $B^0 \rightarrow p\bar{p}K_S$, after the application of the charm

and Λ_c vetoes, no significant signal is observed in either the ΔE or M_{bc} distribution. A fit to the ΔE distribution gives $6.4^{+4.4}_{-3.7}$ events. Applying the Feldman-Cousins procedure [13], we obtain an upper limit of less than 16 events at the 90% confidence level (C.L.). After reducing the detection efficiency by the systematic error, we obtain an upper limit at 90% C.L. of $\mathcal{B}(B^0 \rightarrow p\bar{p}K^0) < 7.2 \times 10^{-6}$.

In the $B^+ \rightarrow p\bar{p}\pi^+$ mode, after the application of the charm veto we perform a fit to the ΔE distribution that allows for $B^+ \rightarrow p\bar{p}\pi^+$ signal and a reflection from misidentified $B^+ \rightarrow p\bar{p}K^+$ decays. This fit gives a signal yield of $16.2^{+8.6}_{-8.0}$ events and a significance of 2.1σ . The excess in the ΔE fit corresponds to a branching fraction $\mathcal{B}(B^+ \rightarrow p\bar{p}\pi^+) = (1.9^{+1.0}_{-0.9} \pm 0.3) \times 10^{-6}$ or an upper limit of $\mathcal{B}(B^+ \rightarrow p\bar{p}\pi^+) < 3.7 \times 10^{-6}$ at 90% C.L. after taking into account the systematic error.

We have observed a significant signal (5.6σ) for the decay $B^+ \rightarrow p\bar{p}K^+$. This is the first $b \rightarrow s$ decay mode with baryons in the final state. In the future, this mode can be used to search for direct CP violation [2]. We find that its $p\bar{p}$ mass spectrum is inconsistent with phase space and is peaked toward low mass. This feature is suggestive of quasi two-body decay. It is also possible that the decay is a genuine three-body process and that this feature of the $M(p\bar{p})$ spectrum is a baryon form factor effect [14,15].

We wish to thank the KEKB accelerator group for the excellent operation of the KEKB accelerator. We acknowledge support from the Ministry of Education, Culture, Sports, Science, and Technology of Japan and the Japan Society for the Promotion of Science; the Australian Research Council and the Australian Department of Industry, Science and Resources; the National Science Foundation of China under contract No. 10175071; the Department of Science and Technology of India; the BK21 program of the Ministry of Education of Korea and the CHEP SRC program of the Korea Science and Engineering Foundation; the Polish State Committee for Scientific Research under contract No. 2P03B 17017; the Ministry of Science and Technology of the Russian Federation; the Ministry of Education, Science and Sport of Slovenia; the National Science Council and the Ministry of Education of Taiwan; and the U.S. Department of Energy.

-
- [1] Hereafter, the inclusion of the charge conjugate mode is implied.
 - [2] G. Eilam, M. Gronau, and J. Rosner, Phys. Rev. D **39**, 819 (1989).
 - [3] X. Fu *et al.* (CLEO Collaboration), Phys. Rev. Lett. **79**,

3125 (1997).

- [4] T.E. Coan *et al.* (CLEO Collaboration), Phys. Rev. D **59**, 111101 (1999). CLEO also carried out a search for non-resonant $B^+ \rightarrow p\bar{p}K^+$ and found that its branching fraction was less than 8.9×10^{-5} ; T. Bergfeld *et al.* (CLEO Collaboration), Phys. Rev. Lett. **77**, 4503 (1996).
- [5] H. Albrecht *et al.* (ARGUS Collaboration), Phys. Lett. B **209**, 119 (1988).
- [6] P. Abreu *et al.* (DELPHI Collaboration), Phys. Lett. B **357**, 255 (1995); W. Adam *et al.* (DELPHI Collaboration), Z. Phys. C **72**, 207 (1996).
- [7] K. Abe *et al.* (Belle Collaboration), BELLE-CONF-0116, paper submitted to the 2001 Lepton-Photon Conference.
- [8] KEKB B Factory Design Report, KEK Report 95-1, 1995, unpublished.
- [9] A. Abashian *et al.* (Belle Collaboration), *The Belle Detector*, KEK Report 2000-4, to be published in Nucl. Instrum. Methods.
- [10] The regions $2.85 < M(p\bar{p}) < 3.128 \text{ GeV}/c^2$ and $3.315 < M(p\bar{p}) < 3.735 \text{ GeV}/c^2$ are excluded to remove background from modes with $\eta_c, J/\psi$ and $\psi', \chi_{c0}, \chi_{c1}$ mesons, respectively.
- [11] The Fox-Wolfram moments were introduced in G.C. Fox and S. Wolfram, Phys. Rev. Lett. **41**, 1581 (1978). The Fisher discriminant used by Belle is described in K. Abe *et al.*, Phys. Rev. Lett. **87**, 101801 (2001) and K. Abe *et al.*, Phys. Lett. B **511**, 151 (2001).
- [12] D.E. Groom *et al.* (Particle Data Group), Eur. Phys. J. C **15**, 1 (2000).
- [13] G.J. Feldman and R.D. Cousins, Phys. Rev. D **57**, 3873 (1998).
- [14] C.-K. Chua, W.-S. Hou, and S.-Y. Tsai, hep-ph/0108068 to appear in Phys. Lett. B; Phys. Rev. D **65**, 034003 (2002).
- [15] H.-Y. Cheng and K.-C. Yang, hep-ph/0112245.